Scripta Materialia 146 (2018) 286–289

Contents lists available at ScienceDirect

Scripta Materialia

journal homepage: www.elsevier.com/locate/scriptamat

Regular article

Quantification of local mobilities

Y.B. Zhang

Department of Mechanical Engineering, Technical University of Denmark, 2800 Kgs. Lyngby, Denmark

ARTICLE INFO

Article history:
Received 12 September 2017
Received in revised form 24 November 2017
Accepted 12 December 2017
Available online xxxx

Keywords:
Mobility
Recrystallization
Grain boundary migration
Electron backscatter diffraction (EBSD)
Electron channeling contrast (ECC)

ABSTRACT

A new method for quantification of mobilities of local recrystallization boundary segments is presented. The quantification is based on microstructures characterized using electron microscopy and on determination of migration velocities and driving forces for local boundary segments. Pure aluminium is investigated and the results show that even for a single recrystallization boundary, different boundary segments migrate differently, and the differences can be understood based on variations in mobilities and local deformed microstructures. The present work has important implications for understanding of recrystallization boundary migration, and suggests an experimental way forward for how to determine boundary mobilities during recrystallization.

The migration of recrystallization boundaries is typically expressed by the equation:

$$v = MF \tag{1}$$

where v is the migration velocity, M is the boundary mobility and F is the driving force for migration, which for recrystallization is the energy stored in the deformed matrix [1]. Recent new results show that locally the migration of recrystallization boundary segments is very heterogeneous both in time and space: the recrystallization boundary is rough consisting of local protrusions/retrusions and migrates in a stop-go fashion [2–5]. Quantitative analysis of local boundary migration has suggested that the boundary mobilities for *local* boundary segments have to be known in order to understand this heterogeneous process [4,5].

Several results have been published on boundary mobilities during recrystallization, e.g. [6–11]. However, these results are averaged over groups of grains, as the driving force used in these studies is that for the whole sample. It is now well recognized that the deformed microstructure varies from grain to grain [12,13], and that variations typically also exist within individual grains. The local driving force is therefore expected to vary both on the grain scale and the subgrain scale. These variations have not yet been taken into account for analysis of boundary migration during recrystallization.

The aim of the present study is to propose a method to derive *local mobilities* of boundary segments at different places along a recrystallizing boundary and thus to take the local microstructural variations into account. The method is based on a quantification of the local deformation microstructures that provides the driving force for the local boundary migration, and of local migration velocities. When the purpose is to understand the local boundary migration, the results confirm that it is absolutely necessary to focus on the local deformed microstructure, as even nearby boundary segments on the same boundary behave differently when migrating into the neighboring deformed matrix.

High purity aluminium (99.996%) with a large initial grain size of several millimeters was cold rolled to 50% reduction in thickness, followed by annealing at 250 °C for 10 min to create a partially-recrystallized microstructure. The sample was electropolished for scanning electron microscope (SEM) analysis to allow selection of a recrystallization boundary. The sample was then annealed 6 times at 250 °C for 15 min in an air furnace to follow the migration of the selected recrystallization boundary. After each annealing step, the microstructure was characterized using the electron channeling contrast (ECC) technique in a Zeiss Supra SEM, without any additional surface treatment. The microstructure after the first ex-situ annealing step (i.e. the first 15 min annealing) was also characterized using the electron backscatter diffraction (EBSD) technique with a step size of 0.5 μm for quantification of local stored energies. During the EBSD scan thermal and mechanical drift of the electron beam and/or the sample as well as geometrical misalignment of the sample [14] induce spatial distortion in the EBSD maps. These spatial distortions in the EBSD map were corrected using the thin plate spline method described in [15] (see details in section A in the supplementary material).

The ECC image and EBSD map of the selected boundary are shown in Fig. 1a and b, respectively. They were both taken after the first ex-situ annealing step at 250 °C for 15 min, and this is referred to as the starting boundary position. The ECC image in Fig. 1a shows that the deformed microstructure consists mainly of two sets of dislocation boundaries,

E-mail address: yubz@mek.dtu.dk.

https://doi.org/10.1016/j.scriptamat.2017.12.012
1359-6462/

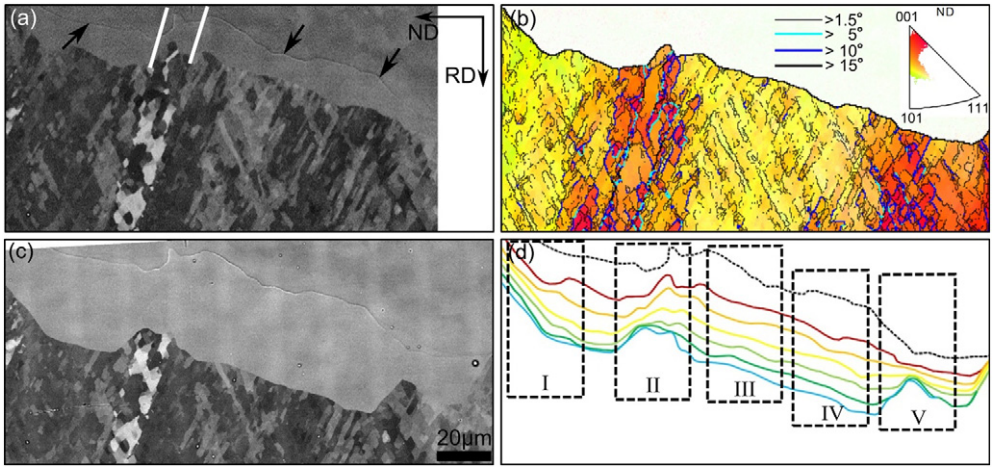

Fig. 1. (a) and (c) are ECC images showing the investigated microstructure at the starting state and after 6 steps of annealing at 250 °C for 15 min each. The black arrows in (a) mark the groove developed during electropolishing, while the white lines mark the large-scale subdivision region. (b) EBSD map showing the same microstructure as that in (a). The colors in (b) represent the crystallographic direction parallel to the sample ND (see the inset). (d) Traces of the recrystallization boundary after each annealing step. Boxes I–V mark five selected regions for local quantitative analysis. The groove seen in (a) and (c) is shown by a dotted line in (d) for reference. (For interpretation of the references to color in this figure legend, the reader is referred to the web version of this article.)

lying at ±25–30° to RD. The spacing of the two sets of dislocation boundaries is about 1–2 μm. A relatively coarse band (~12 μm), representing large-scale subdivision [12] is marked by the white lines. In the EBSD map (Fig. 1b), the large-scale subdivision region appears orange/red, i.e. the crystallographic orientations along the sample normal direction (ND) are closer to ⟨001⟩, compared to the neighboring yellow and yellow-green regions, for which the crystallographic orientations along ND are closer to ⟨012⟩. The microstructure of the coarse band is heterogeneous, consisting of a large number of dislocation boundaries with misorientations >10–15°, while the neighboring yellow and yellow-green regions are more homogeneous, consisting of dislocation boundaries with misorientations mainly <5°. The two sets of dislocation boundaries in the coarse band region are nearly parallel to those in the homogeneous regions. In the coarse band, the set aligned at about +25° to RD is slightly more dominant than the other set, while the two sets of dislocation boundaries in the neighboring yellow and yellow-green regions are similar. The region to the right in the image appears orange-red, i.e. with ND close to <001>, and consists of dislocation boundaries with misorientations in the range 10–15°.

For the quantitative analysis of local boundary migration, the deformed microstructure in front of the migrating boundary is divided into five regions, as marked by the white 25-μm-wide boxes in Fig. 1d. The selection of the boxes is based on the textural (i.e. color in the EBSD map) and microstructural differences: boxes I, III and IV are from the yellow and yellow-green regions where microstructures are relatively homogeneous, while boxes II and V are from orange-red regions where microstructures are more heterogeneous. The orientation variations within the five regions are listed in Table 1.

The position of the recrystallization boundary after the final (6^{th}) annealing step is shown in Fig. 1c. The traces of the recrystallizing boundary after each annealing step are sketched in Fig. 1d based on the ECC images. It is seen that the boundary has migrated mainly along RD. The recrystallizing boundary segments in the central homogeneous regions (in boxes III and IV) are relatively flat and the boundary migration is quite uniform, while the boundary segments in the left heterogeneous region (in box II) are rougher, consisting of many local protrusions and retrusions, and the migration there is non-uniform. A large retrusion has developed in the orange-red region in box V during the last 2 annealing steps, while a large protrusion has developed in the region to the left (in box I).

Table 1
Orientation variation for each of the deformation regions marked by the five boxes in Fig. 1d. Only areas that have been consumed during annealing within each box are included in the calculation.

Boxes	I	II	III	IV	V
Orientation variation	2.0°	10.1°	1.7°	1.8°	4.0°

For quantification of local boundary mobilities using Eq. (1), the migration velocity, v, and driving force, F, of local boundary segments within each of the five boxes in Fig. 1d was determined. Following previous studies [16,17], both the stored energy, F_S, in the deformed microstructure and the driving force attributed to the boundary curvature, F_σ, are quantified and included in total driving force F. For the calculation of the stored energy using the method described in [18,19], the EBSD map was filtered using a 3 × 3 Kuwahara filter to reduce orientation noise [20]. After filtering, most of the dislocation boundaries in the deformed microstructure can be seen (see Fig. S2). Using this filtered EBSD map, all dislocation boundaries with misorientations ≥1° were included in the calculation of F_S. The contribution to the stored energy from the loose dislocation density within the subgrains is not considered, as this contribution is very small compared to that from dislocation boundaries [21]. The variations in v and F for each local segment were also estimated as described in section B in the supplementary materials. The recovery of the deformation matrix during ex-situ annealing is very minor (see section C in the supplementary materials) and is not considered in the calculation of F_S.

The results are shown in Fig. 2. It is evident that the local boundary segments in the five boxes migrate quite differently. Two general trends can, however, be summarized. Firstly, homogenous regions lead to relatively homogenous migration and vice versa: the variations of v (the vertical error bars in Fig. 2) are relatively small for boundary segments in boxes I, III and IV (in the range 0.02–0.07 μm/min), compared to those for boundary segments in boxes II and V (in the range 0.08–0.13 μm/min). The observed differences are directly related to the fact that the variation of F (the horizontal error bars in Fig. 2) is relatively small within the homogenous regions (boxes I, III and IV), in the range 0.02–0.05 MJ/m^3, compared to those for heterogeneous regions (boxes II and V), in the range 0.07–0.15 MJ/m^3. Secondly, on a local scale both average migration velocity and driving force vary from time to time, even for the boundary segments within the homogenous regions: The average value of v is in the range of 0.10–0.41 μm/min, and the average value of F is in the range of 0.07–0.3 MJ/m^3.

For quantification of the mobilities, a linear fitting to Eq. (1) has been performed for the data in each region. The fitting is forced to go through the origin. As shown in Fig. 2, after taking the variations of measured v